Cognitive Neurodynamics (2021) 15:661–674
https://doi.org/10.1007/s11571-020-09655-w

RESEARCH ARTICLE

Automated detection of schizophrenia using optimal wavelet-based l_1 norm features extracted from single-channel EEG

Manish Sharma[1] · U. Rajendra Acharya[2,3,4]

Received: 22 July 2020 / Revised: 12 November 2020 / Accepted: 27 November 2020 / Published online: 15 January 2021

Abstract

Schizophrenia (SZ) is a mental disorder, which affects the ability of human thinking, memory, and way of living. Manual screening of SZ patients is tedious, laborious and prone to human errors. Hence, we developed a computer-aided diagnosis (CAD) system to diagnose SZ patients accurately using single-channel electroencephalogram (EEG) signals. The EEG signals are nonlinear and non-stationary. Hence, we have used wavelet-based features to capture the hidden non-stationary nature present in the signal. First, the EEG signals are subjected to the the wavelet decomposition through six iterations, which yields seven sub-bands. The l_1 norm is computed for each sub-band. The extracted norm features are disseminated to various classification algorithms. We have obtained the highest accuracy of 99.21% and 97.2% using K-nearest neighbor classifiers with ten-fold and leave-one-subject-out cross-validations. The developed single-channel EEG wavelet-based CAD model can help the clinicians to confirm the outcome of their manual screening and obtain an accurate diagnosis.

Keywords Schizophrenia · EEG · Computer-aided diagnosis (CAD) · KNN

Introduction

The brain controls the functions of the human body, and its malfunctioning may impact normal behaviour and activities. Any mental disease or disorder can change the human psychic abilities of thinking, decision making. The schizophrenia(SZ) can be regarded as a psychological ailment which adversely influences the thinking, feeling and actions (Laursen et al. 2013). According to the WHO report, SZ is a critical mental health illness, and approximately 2.1 crore people are affected (Laursen et al. 2013). Yet, the exact cause and treatment are not available (Laursen et al. 2013). It is treated generally in stages, early or post-diagnosis can help to determine its intensity. The detection and treatment of SZ are necessary, as it severely affects the quality of living. If left untreated, it can become a terrible disease, which may damage the human behaviour in its subsequent phases. Early diagnosis of SZ, may help in getting proper treatment and prevent from worsening the condition.

Mostly, mental disorders are assessed using physiological signals or questionnaire techniques (Acharya et al. 2015, 2018b). But nowadays, electroencephalogram (EEG) signals are widely used to detect the brain related diseases as they are easy to acquire using multi-channel sensor array and also economical (Ibáñez-Molina et al. 2018; Li et al. 2008; Sharma et al. 2020). The classification accuracy of SZ depends upon the tools used to examine these signals. The imaging techniques, such as computed tomography (CT) and magnetic resonance imaging (MRI), are costly and take more time to record and process the images as compared to EEG signals (Subudhi et al. 2018; Talo et al. 2019; Gudigar et al. 2019; Acharya et al. 2012). The

✉ Manish Sharma
manishsharma.iitb@gmail.com; manishsharm@iitram.ac.in

U. Rajendra Acharya
aru@np.edu.sg

[1] Department of Electrical and Computer Science Engineering, Institute of Infrastructure Technology Research and Management, Ahmedabad, India

[2] Department of Electronics and Computer Engineering, Ngee Ann Polytechnic, Singapore, Singapore

[3] Department of Biomedical Engineering, School of Science and Technology, Singapore University of Social Sciences, Singapore, Singapore

[4] Department of Bioinformatics and Medical Engineering, Asia University, Taichung City, Taiwan, ROC

electrical activity of the neurons contributes to the synaptic release and the neuronal signalling. These electrical shifts are sudden, of a millisecond or even micro-second order, with small amplitude (order of microvolts). EEG signals are acquired by placing electrodes at different positions of the scalp according to 10–20 international standards. These EEG signals can be used to analyze different diseases such as Parkinson's disease (Bhurane et al. 2019a), sleep disorder (Sharma et al. 2018b, d, 2019a, b; Dhok et al. 2020), dementia, SZ, Alzheimer's disease, and other mental disorders (Yıldırım et al. 2018; Tripathy and Acharya 2018; Acharya et al. 2018c; Sharma and Acharya 2018; Sharma et al. 2018a, e). In this work, we have proposed a CAD model for the detection of schizophrenia, as this process is faster and more accurate than the other detection methods. Automated SZ detection using EEG signals may increase the speed, and accuracy of diagnosis. It may also reduce possible human errors.

Recent studies provide insights into automated SZ classification using EEG signals. Kim et al. (2015) analyzed EEG obtained from electrode cups positioned as per 10–20 international standards. They got five frequency bands, and computed power of every band using fast Fourier transform (FFT). The highest accuracy of 62.2% using the delta band. However, Dvey-Aharon et al. (2015) incorporated the Stockwell approach for EEG-image conversion, and time-frequency transformation is performed on the EEG signals. They have received the classification accuracy between 91.5 and 93.9% for top five electrodes. Johannesen et al. (2016) used a 64 electrode system to obtain the EEG recordings. The response given by participants is analyzed and segmented via four-stage processing. Time-frequency data for each of five frequency bands are computed. The spectral power for frontal, central and occipital locations are statistically analyzed. They developed two models for classification. The first model is developed to discriminate correct and incorrect trials and achieved an accuracy of 87%. The second model is used to further classify the correct trial data into normal vs SZ condition and achieved an accuracy of 87% using support vector machine (SVM). Santos-Mayo et al. (2016) used brain vision equipment to record the EEG signals. After EGG-LAB preprocessing, 16 features are obtained per electrode per participant and classified using the multilayer perceptron (MLP) and SVM classifiers. They have obtained 93.42% and 92.23% accuracy for J5 MLP (multi layer perceptron) and J5 SVM classifiers (Devijver and Kittler 1982). Ibáñez-Molina et al. (2018) have carried out EEG-based SZ assessments. The resting EEG from participants are used in this study and involved in a naming activity. For data acquisition the Neuroscan SynAmps 32-channel amplifier is used. EEG signals are collected and segmented. The segments are analyzed by moving a window over the entire EEG recording during the resting stage. Subsequently, Lempel-Ziv complexity (LZC) is was measured per window. The final LZC value is determined after standardization by measuring the sum of all values obtained from each window. At the task, a group of 80 EEG segments are analyzed and then summed for the final multiscale LZC score. Patients who have been resting provided higher complexity scores in right frontal zones. Oh et al. (2019), suggested a deep learning-based system to discriminate SZ using EEG signals, automatically. They have proposed convolutional neural network (CNN) based model with ten-fold cross-validation and blind-fold validation strategies. They reported accuracy of 81.26% for blind-fold strategy and 98.07% for ten-fold cross-validation strategy. Recently, Siuly et al. (2020) have introduced SZ detection using statistical features obtained from intrinsic modes of EEG multi-channel signals. They succeed in attaining 93.2%. Vicnesh et al. (2019), developed a CAD to classify normal and SZ classes using non-linear features extracted from EEG segments. They have reported an accuracy of 92.91% using an SVM classifier with 12 features. Our proposed CAD system is shown in Fig. 1. The EEG recordings are segmented into epochs of 25 s. Then they are subjected to an optimal root-mean-squared frequency spread minimized (RMSFSM) orthogonal wavelet filter bank (Sharma et al. 2018c, 2019c, e). The l_1 norm features are computed for each of seven sub-bands, which are obtained from the six-level wavelet decomposition of EEG segments. Then the features are fed to several classifiers, including ensemble subspace k-nearest neighbor (KNN) classifier. The salient features of the proposed study are as follows:

1. We have developed single-channel EEG based system whereas most of the existing systems (Siuly et al. 2020; Oh et al. 2019; Vicnesh et al. 2019; Moulin et al. 1997; Akar et al. 2012) are based on a multiple-channel system. Hence, our system is simple, portable and convenient to patients.
2. Simulation results reveal that the proposed model obtains unity value of AUC, an F1 score of 0.99, and accuracy of 99.21% using a single channel Cz-channel alone. Hence, the system is accurate and less complex.
3. In this study, we have used only seven wavelet-based discriminating features. Thus the cost of computation of the proposed model is less.
4. In the proposed work, we have deployed a new class of an optimal two-band orthogonal wavelet filter bank called RMSFSM, wherein filters are optimally localized in the frequency domain.
5. The proposed model performs well in terms of classification performance.

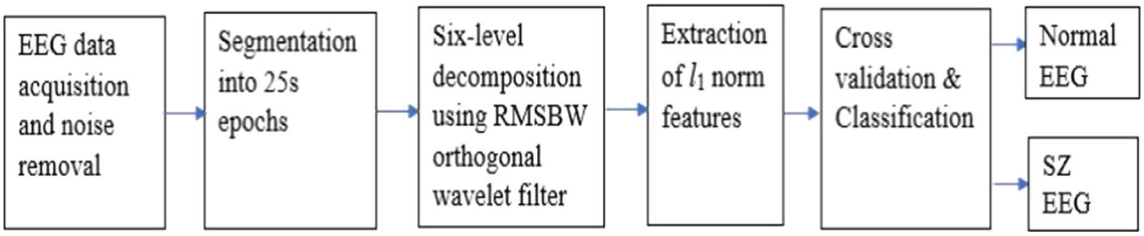

Fig. 1 Proposed process flow diagram. First, all EEG signals were acquired from 19 electrodes viz. T4, T6, Fp2, F8, Fp1, F7, F4, Fz, T3, T5, O1, O2, C4, P4, P3, F3, C3, Cz, and Pz are preprocessed by passing through the Butterworth filter of order six. The digitized EEG records of all 19 electrodes are then segmented into epochs of the length 25 s. Then epochs corresponding to each of 19 channels are applied to the designed optimal RMSFMS filter. Wavelet decomposition yielded various subbands of the EEG epochs. Subsequently, the l_1 norm features of each subband is computed. These features are applied to various machine learning classifiers for the classification of epochs as normal or SZ

6. To ensure the model's robustness and avoid possible over-fitting, we have used ten-fold, leave-one-subject-out cross-validations (LOSOCV), and hold out validation. All strategies gave a comparable performance.

Data-set

The EEG signals were obtained from 14 paranoid SZ patients (7 females + 7 males), with an average age of 28.3 ± 4.1 and 27.9 ± 3.3 years, respectively. Data was obtained from the institute of psychiatry and neurology in Warsaw, Poland (Olejarczyk and Jernajczyk 2017). The EEG signals were recorded with eyes-closed and in resting state on a multi-channel(19-channels), at a sampling frequency of 250 Hz. Electrodes used were T4, T6, Fp2, F8, Fp1, F7, F4, Fz, T3, T5, O1, O2, C4, P4, P3, F3, C3, Cz and Pz. The EEG signal from Cz-channel of a normal and SZ patient is shown in Fig. 2 and 3, respectively. Table 1 provides the details of the data-set used for this work. Figures 4 and 5 show the 19-channel EEG signals corresponding to the normal and SZ classes, respectively.

Proposed method

In this paper, 15-min EEG signals are sampled at 250 Hz and pre-processed using sixth-order Butterworth filter. Then signals are segmented into 25 s non-overlapping segments giving 516 normal and 626 SZ segments. The details of data used is given in Table 1.

Optimal design of FBs

Though the Fourier transform (FT) is considered as a promising tool for analyzing non-stationary and time-invariant events, it is not suitable for the analysis of phenomena, which are time-varying and non-stationary (Sharma et al. 2010, 2015, 2016). This shortcoming of FT can be overcome by short time Fourier transform (STFT) by analyzing the signal into small slices to gather the information required (Sharma et al. 2017b; Bhati et al. 2016; Rajput et al. 2019). The main disadvantage for STFT is that the signal width to be measured as a small portion is unchanged and therefore, details must be collected in both low and high-frequency sections. The most important tool that provides the information about a signal in both time and the frequency domains simultaneously is called the wavelet (Rajendra et al. 2018; Sharma et al. 2017a, c). The

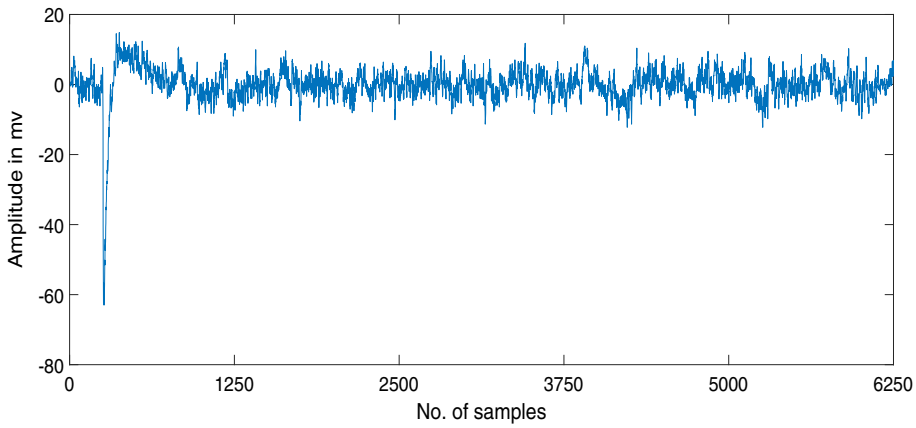

Fig. 2 Sample EEG signal obtained from Cz-channel of normal subject. X axis represents sample-index and Y axis represents magnitude in mV

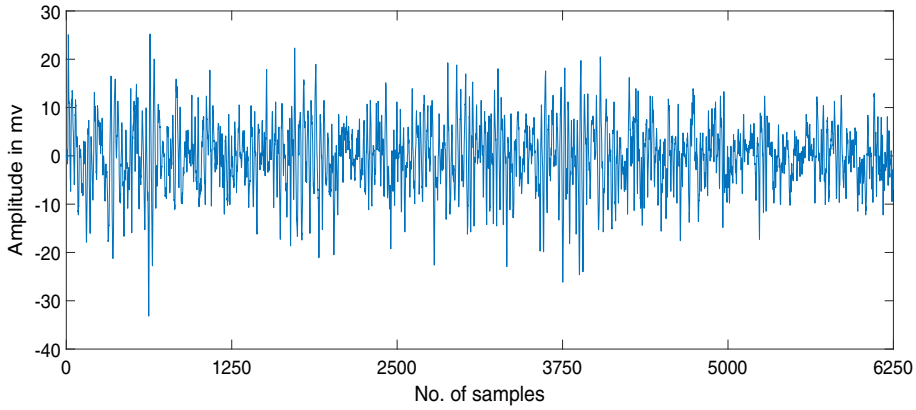

Fig. 3 Sample EEG signal obtained from Cz-channel of SZ patient. X axis represents sample-index and Y axis represents magnitude in mV

Table 1 Details of dataset used in this study

Class	No. of subjects	Avg. age of M and F in years	Total no. epochs
Normal	14(7M + 7F)	26.8 ± 2.9, 28.7 ± 3.4	516
SZ	14(7M + 7F)	27.9 ± 3.3, 28.3 ± 4.1	626

The EEG signals are recorded for 19 electrodes, namely T4, T6, Fp2, F8, Fp1, F7, F4, Fz, T3, T5, O1, O2, C4, P4, P3, F3, C3, Cz, and Pz. The sampling frequency of EEG signals is chosen 250 Hz to digitize the EEG recordings. The duration of each epoch is 25s; thus, each epoch contains 6250 samples

M Male, *F* female, *SZ* schizophrenia

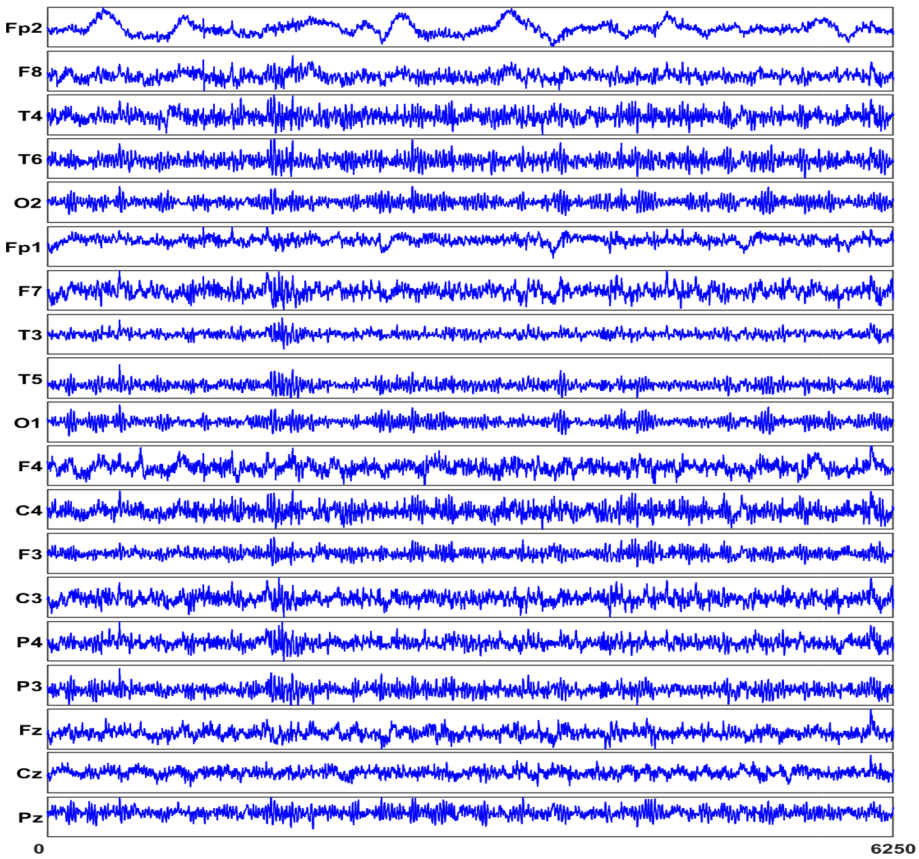

Fig. 4 19-Channel EEG segments of a normal subject. Y-axis represents EEG electrodes Fp2, F8, T4, T6, O2, Fp1, F7, T3, T5, O1, F4, Fz, C4, P4, P3, F3, C3, Cz, and Pz. X-axis: no. of samples at sampling frequency 256

wavelet magnifies the signal into tiny windows so that the required information can be obtained by scaling and shifting process. A narrow window is utilized during high-frequency analysis and the wider window is used to

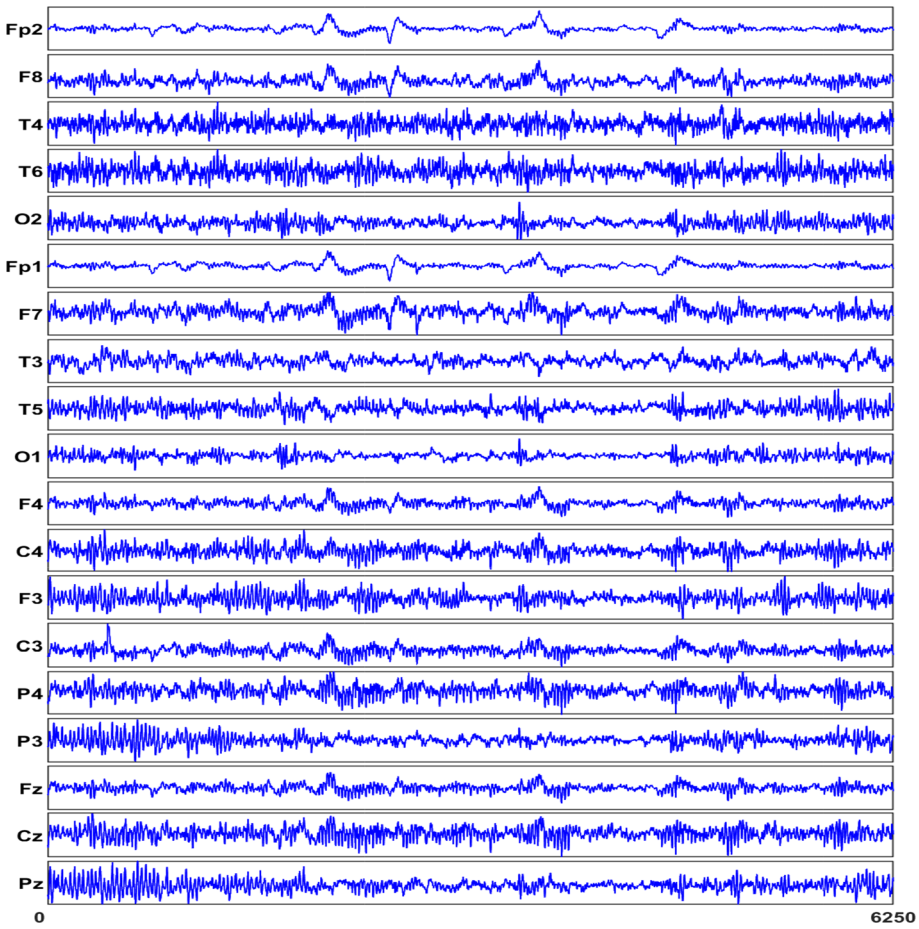

Fig. 5 19-Channel EEG segments of SZ patient. Y-axis: EEG electrodes Fp2, F8, T4, T6, O2, Fp1, F7, T3, T5, O1, F4, Fz, C4, P4, P3, F3, C3, Cz, and Pz. X-axis: no. of samples

analyze the low-frequency components (Sharma et al. 2017d; Sharma and Pachori 2017). For signal analysis, two orthogonal channel filter is used. The typical structure of two-band OWFB is shown in Fig. 6. As the optimal criteria, mean-squared-frequency-spread (MSFS) of the filters is used as, for constructing finitely supported orthogonal wavelet filter banks (OWFB) (Shah et al. 2019; Sharma et al. 2018f; Sharma and Acharya 2019), in this work. The optimal RMSFMS filters used in this work have minimum frequency spread and the desired number of zero moments (Tay et al. 2014; Sharma et al. 2019e), which are essential for generating smooth wavelets. The RMSFMS FBs were found to be performing well in applications of image compression and signal de-noising (Sharma et al. 2017c). Tay et al. (2014) noticed that RMSFMS filters exhibit better performance than other orthogonal counterparts in image processing applications. Sharma et al. (2017b, 2020) showed that RMSFMS localized filter banks perform well in the analysis of EEG and ECG signals. Thus, frequency localization is an important attribute in selecting and designing optimal filters and FBs. RMSFSM filter used in this study possesses the following features. (1) Unlike the traditional filter design techniques, one does not require to mention cutoff frequencies corresponding to the stop passbands. (2) The RMS bandwidth can be considered a good measure of the filter's frequency localization. The

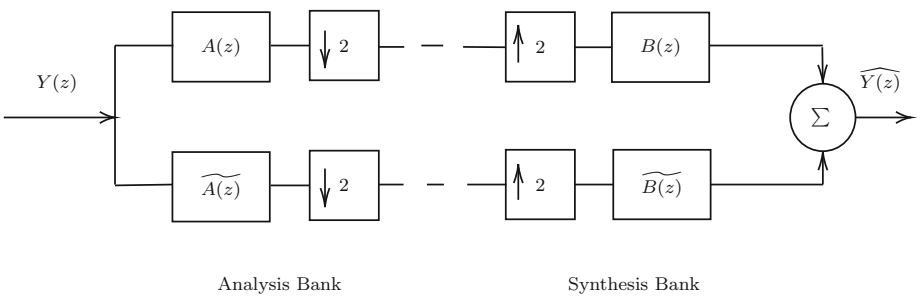

Fig. 6 Typical structure of two band OWFB, $A(z)$ and $\widetilde{A(z)}$ are analysis lowpass and highpass filters, simialrly $B(z)$ and $\widetilde{B(z)}$ represent synthesis lowpass and highpass filters

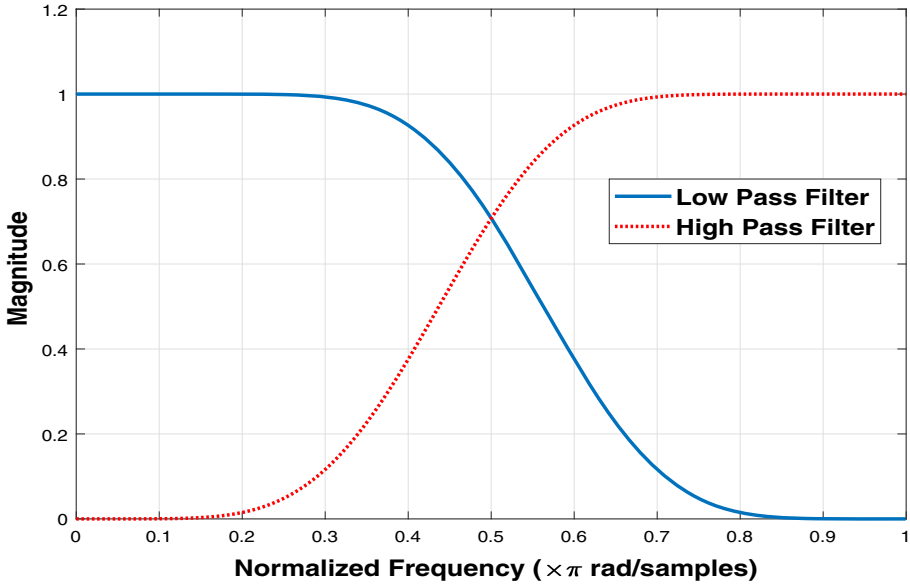

Fig. 7 Magnitude response of designed filter pair, where y-axis represents magnitude and x-axis represents normalized frequency in rad/sample

RMS BW takes care of the entire spectrum. (3) The RMSFMS filters have significantly fewer ripples and sharp roll-off (Sharma et al. 2019d).

Figure 6 shows a two-band filter bank, where low-pass filter (LPF) $A(z)$, high-pass filter (HPF) and $\widetilde{A(z)}$, and low-pass filter $B(z)$, high-pass filter $\widetilde{B(z)}$ are used in analysis and synthesis banks, respectively. The output of each filter is down-sampled by a factor of 2 in the analysis bank whereas in synthesis bank it is up-sampled by a factor of 2. The time-reversed version of high and low pass filters in the analysis bank gives the respective filters in synthesis bank. High pass filters in OWFB are obtained by quadrature conjugation of respective low pass filters (Vetterli et al. 1992). As a result, by designing one filter, one can get the other three filters. Generally, filters $B(z)$, $\widetilde{A(z)}$ and $\widetilde{B(z)}$ are designed with the help of $A(z)$ filter of analysis bank. The product filter $F(z) = A(z)B(z) = A(z)A(z^{-1})$ must satisfy the below condition to get OWFB (Vetterli et al. 1992; Daubechies 1992).

$$F(z) + F(-z) = 2 \text{ (Half Band Condition)} \tag{1}$$

Here, $F(z) = A(z)B(z)$ is the product filter, and $A(z)$ & $B(z)$ are the analysis and synthesis lowpass filters of the FB shown in Fig. 6.

To design optimal filters $A(z)$ and $B(z)$ of the underlying OWFB, we design half-band filter $F(z)$ first with constraints of the non-negativity and regularity. The desired LPFs $A(z)$ and $B(z)$ have been retrieved through the spectral factorization of $F(z)$ (Bhurane et al. 2019b). The unit impulse response sequences of analysis LPF $A(z)$ and the synthesis LPF $B(z)$ are denoted as $a(n)$ and $b(n)$, $0 \le n \le L-1$. The optimization criterion for designing the orthogonal FB is to minimize the MSFS of the LPFs. Since, both $A(z)$ and $B(z)$ have same MSFS. Minimizing the MSFS of $A(z)$ also results in minimizing the MSFS of $B(z)$. The MSFS α_ω^2 of low pass filter $A(z)$ is given by (Sharma et al. 2018c)

$$\alpha_\omega^2 = \frac{1}{2\pi E}\int_{-\pi}^{\pi} \omega^2 |A(e^{j\omega})|^2 d\omega \tag{2}$$

where, E is the squared L_2 norm of the sequence $a(n)$, and $A(e^{j\omega})$ represents the discrete time Fourier transform of the sequence $a(n)$. The filter $A(z)$ satisfies orthogonality and regularity. The optimization problem, with degree of regularity of M, can be formulated as follows :

$$\underset{a[n]}{\text{minimize}}\ \alpha_\omega^2 = \frac{1}{2\pi E}\int_{-\pi}^{\pi} \omega^2 |A(e^{j\omega})|^2 d\omega \tag{3}$$

subjected to

Table 2 Filter coefficients of optimal LPF used in this study

Index	Coefficients
1	0.1115
2	0.4946
3	0.7511
4	0.3152
5	− 0.2262
6	− 0.1297
7	0.0975
8	0.0275
9	− 0.0315
10	0.00055
11	0.00477
12	− 0.0011

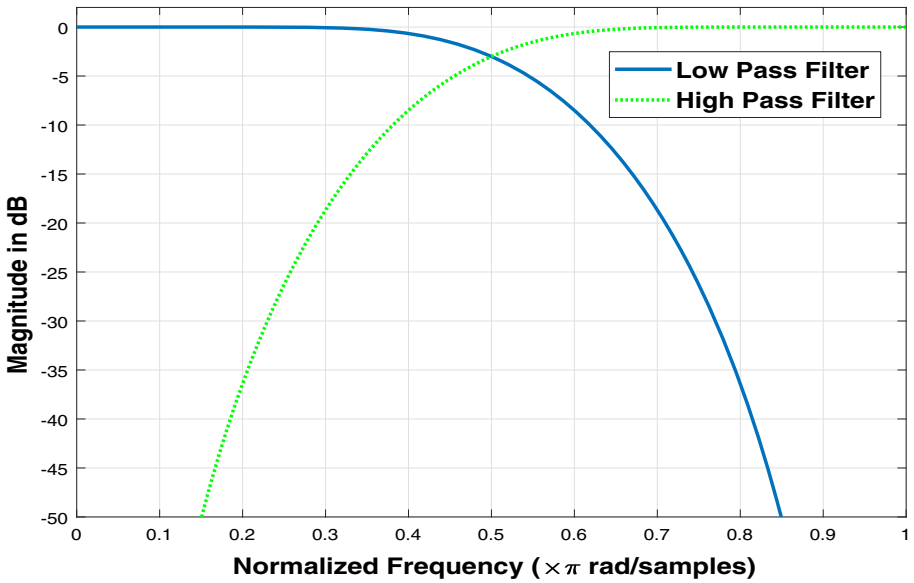

Fig. 8 Frequency response of designed filter pair, where y-axis represents magnitude in dB and x-axis represents normalized frequency in rad/sample

Table 3 Summary statistical properties of seven features extracted from the seven sub-bands yielded by RMSFMS filter bank using the Cz EEG electrode

Sub-band	Normal (mean± std)	SZ (mean± std)	t-value
3	3472.4 ± 920.20	17085 ± 18846	18.046
2	3261.7 ± 1215.4	8489.7 ± 8498.0	15.2048
4	7964.7 ± 2268.1	10923 ± 4435.2	14.538
7	6857.6 ± 1397.6	11170 ± 8424.0	12.60
6	9783.2 ± 3107.7	13063 ± 6681.6	10.93
1	10314 ± 2289.5	21693 ± 39193	7.248
5	16154 ± 8326.8	18094 ± 6411.4	4.337

For the statistical analysis student's test is used with a significance threshold of (0.0001). All features have p vales ($p < 0.0001$). The first columns present the rank of all seven features, second and third columns give mean and std of the corresponding feature for normal and SZ epochs, respectively, used in the study. the last columns present the t value

$$\sum_{n=0}^{L} a(n)a(n-2i) = \delta(i); \quad i = 0, 1, \cdots \frac{L}{2} - 1 \tag{4}$$

$$\sum_{i=0}^{L} (-1)^i i^l a(i) = 0; \quad l = 0, 1, 2, \cdots M - 1 \tag{5}$$

where L and M represnt the length and order of regularity of the lowpass filter $A(z)$.

The optimization problem has been solved using Matlab-based convex optimization toolbox called CVX (Sharma et al. 2014, 2019e). In this work, we used an MSFS optimized filter of order 11 that has five zero moments. The optimal LPF and HPF possess MSFS α_ω^2= 0.8679. The filter coefficients corresponding to optimal LPF are mentioned in Table 2. The optimally designed filter is used in wavelet decomposition of EEG signal. Figures 7 and 8 depict of the frequency responses of the optimal filters.

Features used

The l_1 norm feature of subbands has been computed in this work. The l_1 norm can be simply calculated as the sum of the absolute values of samples of the subband sequence $x(n)$ given by (Wang et al. 2014):

$$l_1(x) = \sum_{n \in \mathbb{Z}} |x(n)| \tag{6}$$

where n is the index of the sequence $x(n)$ and $\mathbb{Z}$ denotes the set of integers.

Classification

Different supervised machine learning classifiers have been used in this proposed method to classify SZ and healthy control classes. The classifiers used are ensemble subspace k-nearest neighbors (KNN) (Sun et al. 2007; Xu et al. 2013), ensemble bagged tree (EBT) (Dietterich 2000), ensemble boosted tree (Dietterich 2000), logistic regression (Tomioka et al. 2007), and SVM (Virdi et al. 2016).

Training, testing and validation

In this work, the data set used is acquired from multiple channels (19-channel). For each EEG epoch, seven l_1 norm features corresponding to the seven SBs, are computed. Hence, the feature vector set contains seven norm features. Firstly, we have tested each channel separately, i.e., we

took all seven features 19 different single-channel EEG signal for classification using ten fold cross-validation (CV). In ten-fold cross-validation, the entire feature dataset is divided into almost ten equal sub-samples. The nine sub-samples are used for model training, and the remaining portion is used for testing. The cycle is repeated ten times so that the training and testing phases are applied to all ten-folds (Fushiki 2011).

For the above-mentioned classification algorithms are employed for all 19 channels, separately. The channel (Cz) that gave the best performance, subsequently chosen for further validation using leave-one-out cross-validation (LOSOCV) and hold out validation. In LOSOCV, 27 subjects out of 28 were used to train the model, and the remaining one used for testing the model. The process was repeated for all 28 subjects. To ensure the robustness, we also performed hold-out validation for the Cz channel that gave the best performance using the ten-fold CV. In this validation, the dataset is split up into the training and testing subsets. In this method, 10%, 20%, 30%, 40% and 50% hold-out are used. In the 10% hold-out, 90% data of the dataset was used as a training set, and the remaining 10% dataset is used as a testing subset. Similarly, in 20%, 30%, 40%, and 50% hold-out 20%, 30%, 40%, and 50% data used as test data respectively, and remaining data used to train the model.

Results

We designed the proposed CAD using Intel(R) Xeon(R) CPU E3-1245 v5 @ 3.50 GHz with 16.0 GB RAM and 64-bit operating system, x64-based processor. The 9.4.0.813654 version of MATLAB R2018a is used. The average feature extraction time for a feature has been 3.173 s.

Features are ranked using student's t-test, which is used to evaluate the quantitative difference between the averages of two groups (De Winter 2013). The t-value is used to measure the measurements of the variation compared to the difference in the specimen data. The t-value indicates whether the two classes are significantly different or not. Higher the t-value higher will be the discriminating potential or rank of the given feature. The p-value is the median sense point within a mathematical hypothesis test which reflects the likelihood of a given event happening. If the p-value corresponding to the given feature found to be lesser than the significance level (.0001) then the null hypothesis can be rejected. Table 3 reflects ranks and t-values corresponding to all features computed for the classification. It is to be noted the values corresponding to each features is less than the threshold value of .0001. Hence, each feature is statistically significant and, therefore, all seven features are utilized for the classification. Since, the number of feature is small there is no need of using any feature reduction/selection techniques.

The average time taken for training and testing is 5.885 s and 50.87 ms, respectively, with the average prediction speed of 2636 obs/s. The classification accuracies for different classifiers using ten-fold CV are shown in Table 4 with the Cz channel. The highest classification performance for the Cz channel using the ten-fold CV is shown in Table 5. We found the average classification accuracy of 99.21% using the ES-KNN classifier with the ten-fold CV. Figure 9 shows receivers operating characteristic (ROC) corresponding to the Cz channel when the classification is performed using all seven features and KNN with ten-fold CV. The ROC presents a variation of the sensitivity with respect to specificity. It is to be noted that our model has attained the perfect unity value of area under the ROC curve (AUC).

The best classification accuracies for remaining 18 channels have also been reflected in Table 6. In order to ensure over-fitting to develop a robust model, we used LOSOCV for the classification using Cz channel. The results of classifications are shown in Table 7 for LOSOCV. From the table, it clear that model achieved the average accuracy of 97.2% and F1-score of 97.42% for KNN with LOSOCV. The confusion matrix and classification results for holdout validation with KNN classifier

Table 4 Summary of best classification results obtained with ten-fold cross validation using Cz channel EEG

CF	CA (%)	PPV (%)	CS (%)	CSF (%)
ES KNN	99.21	98.84	99.42	99.05
KNN	98.77	99.03	98.27	99.20
GSVM	98.42	98.64	97.88	98.87
Bagged trees	98.25	97.48	98.63	97.94
Boosted trees	98.07	98.44	97.32	98.71

The definitions of acronyms used in the table are CF: classifier; ES: ensemble subspace; GSVM: SVM with Gaussian kernel; CA: classification accuracy; CS: classification sensitivity; CSF: classification specificity; PPV: positive predictive value

Table 5 Results obtained for ten-fold CV using Cz channel

Dataset	CA	CS	CSF	F1 score	κ
Whole	99.21%	99.42%	99.05%	99.13%	0.9833
Balanced	98.64%	99.02%	99.02%	98.83%	0.9766

The whole dataset contains 516 and 626 epochs of normal and SZ patients, whereas the balanced dataset contains 516 epochs of each class normal and SZ in the first column. The last column represents cohen's kappa value κ

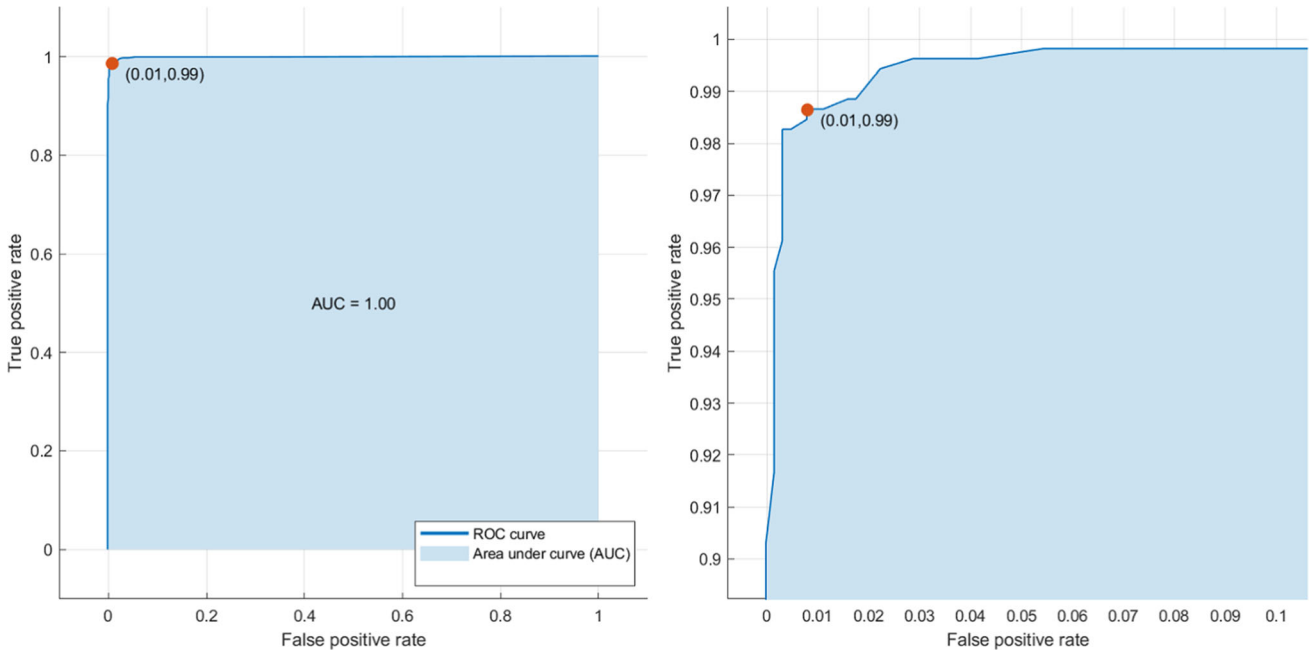

Fig. 9 Left window: ROC for the whole database containing 516 Cz-channel EEG epochs of normal and 626 Cz-channel EEG epochs of schizophrenia patients using KNN classifier with ten fold CV considering all seven features together, Right window: Magnified version of the ROC shown in left window for the false positive rate varying between 0 and 0.1

Table 6 Summary of best classification results obtained with ten-fold cross-validation using each of 19 channels EEG

Channel	CA (%)	PPV (%)	CS (%)	CSF (%)
FP2	91.20	92.90	91.1	91.3
F8	92.2	91.2	91.4	92.8
T4	93.7	93.2	92.8	94.3
T6	95.0	95.5	93.5	96.2
O2	94.1	93.9	93.0	95.0
FP1	96.8	96.9	95.9	97.4
F7	97.6	97.6	97.1	98.0
T3	98.5	99.0	97.7	99.1
T5	98.6	99.2	97.7	99.3
O1	97.7	97.8	97.1	98.2
F4	98.4	98.4	98.0	98.7
C4	98.2	99.0	96.9	99.1
P4	98.7	99.6	97.53	99.6
F3	98.2	98.4	97.5	98.7
C3	96.9	98.6	94.7	98.8
P3	98.6	99.4	97.5	99.5
Fz	97.8	97.2	97.8	97.7
Pz	99.0	98.8	99.0	99.0
Cz	**99.21**	98.84	**99.42**	99.05

The first column represents the electrode used for the classification task. The highest classification accuracy is attained by the Cz channel (in the last row). The bold values represnts the highest values

Table 7 Classification performance for Cz channel using leave one subject out cross vlaidation (LOSOCV)

Classifier	CA	CS	CSF	F1 score
KNN	97.20%	96.49%	98.06%	97.42%

Table 8 Confusion matrix obtained for holdout validation using Cz channel

Holdout (%)	TN	FP	FN	TP
10	50	1	0	63
20	101	2	1	124
30	154	1	1	186
40	204	2	3	247
50	253	5	3	310

In holdout validation, the model is tested by varying the percentage of holdout (testing data) as 10%, 20%, 30%, 40% and 50%, respectively, and the percentage of training data was kept 90%,80%,70%, 60% and 50%, respectively

are shown in Tables 8 and 9, respectively. The best classification accuracy is 99.42% for 30% holdout validation.

It is to be noted that the number of Sz patients and normal subjects is exactly the same (7 SZ and 7 normal).

Though the number of healthy controls and SZ patients are the same, the database appears slightly unbalanced as the number of normal and SZ EEG epochs are not the same. The epochs corresponding to SZ and normal controls are 626 (54.8%) and 516 (45.2%). To take care of the database's slight skewness, we have created a balanced sub-dataset taking 516 random epochs to form each class. Table 5 shows that The classification accuracy of the balanced subset has been found to be 98.64%. Also, the AUC obtained with balanced data is 0.99 (Fig. 10), which is close to the perfect value of 1. Thus, the classification performance corresponding to both (whole and balanced) datasets is almost the same for the Cz channel.

Table 9 Results obtained for holdout validation using Cz channel

Holdout (%)	CA (%)	CS (%)	CSF (%)	F1 score (%)
10	99.12	100	98.44	99.01
20	98.68	99.02	98.41	98.54
30	99.42	99.35	99.47	99.35
40	98.90	98.55	99.20	98.79
50	98.60	98.83	98.41	98.44

In holdout validation, the model is tested by varying the percentage of holdout (testing data) as 10%, 20%, 30%, 40% and 50%, respectively, and the percentage of training data was kept 90%,80%,70%, 60% and 50%, respectively

Discussion

The optimal filter bank was used for wavelet decomposition. In this study, we varied with the decomposition levels between three to seven. After decomposition, features for each wavelet SBs norm feature are computed. We found that the features corresponding to level six were the most dominating that gave the best classification performance. We obtained the best average accuracy of 92.72%, 94.96%, 98.83%, 99.71%, and 97.23% for levels three, four, five, six, and seven for the Cz channel, respectively, using KNN with ten-fold CV. We can see that for the level-six, the accuracy is the highest, followed by the level-five.

It is apparent from Table 3 that the mean value of l_1 of normal EEG signals is comparatively lower than that of the SZ signals for all sub-bands. Also, the standard deviation value of l_1 norm of normal EEG signals is smaller than that of SZ signals for all sub-bands except the fifth sub-band. The amplitude of the SZ EEG signal is higher than the normal EEG signal. Hence, l_1 norm is high in all sub-bands as compared to normal EEG signals. Table 3 provides the details of the best l_1 norm features based on their ranking. These features are used for classification system training

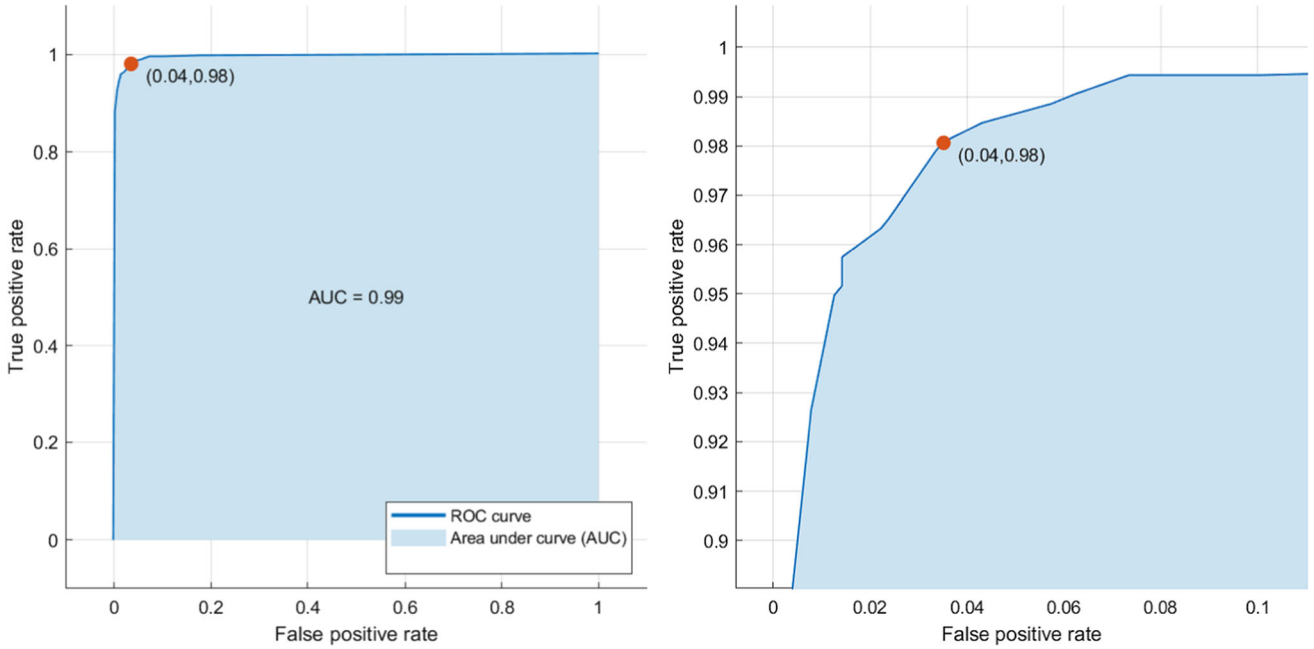

Fig. 10 Left window: ROC for the balanced dataset containing 516 Cz-channel EEG epochs of each normal and schizophrenia patients using KNN classifier with ten fold CV considering all seven features together, Right window: Magnified version of the ROC shown in left window for the false positive rate varying between 0 and 0.1

Table 10 Comparison of our results with the existing automated methods for SZ detection

S. no.	study	Features, method	No. of participants	Dataset	Classification accuracy %	Used electrodes
1.	Kim et al. (2015)	ROC, ANOVA, QEEG parametrs	Normal: 90 subjects Abnornal: 90 patients	Department of Psychiatry, Gongju National Hospital, Korea	62.2	Fp1, Fp2, F7, F3, Fz, F4, F8, T3, C3, Cz, C4, T4, T5, P3, Pz, P4, T6, O1, O2
2.	Dvey-Aharon et al. (2015)	TFT, Feature-Optimisation	Normal: 25 subjects Abnornal: 25 patients	University of A Coruna, Spain	Between 91.5–93.9	F2, Fc3, AFz, FCz, FC5
3.	Johannesen et al. (2016)	SVM	Normal: 12 subjects Abnornal: 40 patients	VA Connecticut Healthcare System (VACHS), Yale	Model 1: 84 Model 2: 87	Fz, Cz, Oz
4.	Santos-Mayo et al. (2016)	MIFS or DISR 15Hz-J5-MLP 35Hz-J5-SVM	Normal: 31 subjects, abnornal: 16 patients	Department of Electrical Engineering, University of Valladolid, Spain	15Hz-J5-MLP: 93.42 35Hz-J5-SVM: 92.23	C3, C4, Cz, F3, F4, F7, F8, Fp1, Fp2, Fz, O1, O2, P3, P4, Pz, T5, T6
5.	Ibáñez-Molina et al. (2018)	DISR, MIFS, J5	Normal: 17 subjects Abnornal: 18 patients	Mental Health Day Hospital of the St Agustín Hospital in Linares	NA	36 Ag/Ag electrodes
6.	Oh et al. (2019)	11-layered CNN Model	Normal: 14 subjects Abnornal: 14 patients	Institute of Psychiatry and Neurology Warsaw, Poland	Non subject specific testing: 98.07 Subject-specific testing: 81.26	Fp1, Fp2, F7, F3, Fz, F4, F8, T3, C3, Cz, C4, T4, T5, P3, Pz, P4, T6, O1, O2
7.	Vicnesh et al. (2019)	SVM, KNN, LD, PNN, DT	Normal: 14 subjects Abnornal: 14 patients	Institute of Psychiatry and Neurology Warsaw, Poland	92.91	Fp1, Fp2, F7, F3, Fz, F4, F8, T3, C3, Cz, C4, T4, T5, P3, Pz, P4, T6, O1, O2
8.	Present work	l_1 Norm, ES-KNN	Normal: 14 subjects Abnornal: 14 patients	Institute of Psychiatry and Neurology Warsaw, Poland	KNN with ten-fold CV: 99.21 KNN with LOSOCV: 97.2	Cz

It is a gene-specific ratio between the mean difference in expression intensity between two groups.It is directly related to Fisher's Linear Discriminant Analysis. It can be defined as the trace of the product of the inter-class dispersion matrix and inverse of the within-class dispersion matrix (Devijver and Kittler 1982); Model 1: correct vs incorrect; Model 2: healthy control vs SZ

ANOVA analysis of variance, *QEEG* quantitative electroencephalography, *TFT* time frequency transformation, *MIFS* mutual information feature selection, *DISR* double input symmetrical relevance, *PNN* probabilistic neural networks, *LZC* lempelaeziv complexity; J5

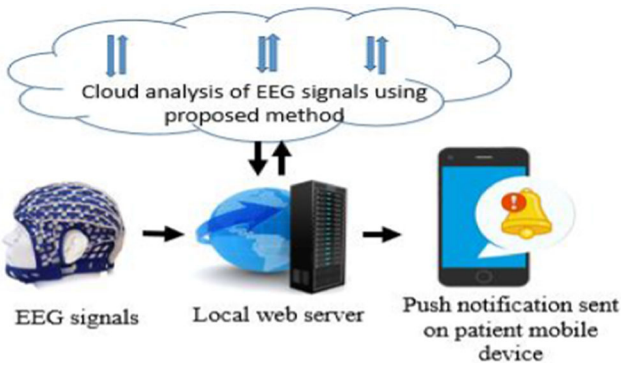

Fig. 11 Design of the proposed cloud model

and testing, which could categorize EEG signals into healthy and SZ classes.

Table 10 provides the summary of automatic systems developed to distinguish normal and SZ EEG signals. Our proposed method reveals that the RMSFSM filter bank based l_1 norm features can efficiently classify SZ and normal EEG signals. It is to be noted that in the table, the first five studies have used different databases than used by the last three studies, including the proposed one. Thus, it is difficult to make a direct comparison of the performance of all studies. Recently, Oh et al. (2019) have developed a deep CNN based automated system to detect SZ using 19-channel EEG signals and obtained classification lower accuracy than our proposed model using the same database.

Also, the computation time required to produce deep learning models is more compared to machine learning models. Moreover, we have achieved comparable classification performance with ten-fold CV, LOSOCV, and hold out validation used by us, and in each case average accuracy was more than 97%. Thus, our proposed model has attained better classification performance than models of Oh et al. 2019; Vicnesh et al. 2019 using the same database. The proposed system used only single-channel EEG, unlike (Kim et al. 2015; Johannesen et al. 2016; Santos-Mayo et al. 2016; Ibáñez-Molina et al. 2018; Oh et al. 2019; Vicnesh et al. 2019) wherein multiple EEG channels were used. Further, Vicnesh et al. (2019) used 12 features, whereas we used only 7 features and obtained better performance than Vicnesh et al. (2019). Hence, the computational cost of the proposed model is lesser than Vicnesh et al. (2019). We have thus obtained better performance than the state-of-art techniques, as reported in Table 10 with the same database.

Main advantages of our proposed method are:

1. Obtained high accuracies of 97.2% and 99.21% using only one single EEG channel with LOSOCV and ten-fold CV. Thus, the model is accurate, as well as robust.
2. Achieved high classification performance for hold validation also.
3. Employed only $l1$ norm-based feature set, which contains seven features extracted from seven wavelet sub-bands.
4. Attained robust system as it is developed with ten-fold.
5. Developed, fast and accurate wavelet-based system.
6. It is obvious from Table 10 that the suggested model succeeds in attaining the highest average classification accuracy and F1 score using only one channel (Cz) EEG. Hence, it reduces the computation time.

Main disadvantages of this method are:

1. Used a small dataset (28 subjects) to develop the model.
2. Duration of EEG signal window is little large (25s).

In future, we can plan to implement deep learning techniques to automatically detect the SZ class without extracting the features (Oh et al. 2018a, b; Acharya et al. 2018a). Also, one can install the proposed CAD system in the cloud to detect the unknown class immediately. Figure 11 illustrates the functioning of the proposed model. Firstly, the EEG signals obtained from patients are stored in the hospital server and sent to the cloud where the proposed wavelet-based model has been installed. The model will analyze the data and detect the SZ immediately. Then the test result is sent from the cloud to the hospital. Then the physician can verify the result manually by comparing his finding with the CAD system.

Conclusion

We have proposed a novel methodology for accurate schizophrenia detection using features extracted from single-channel (Cz channel) EEG. In this model, optimized root-mean-squared-bandwidth orthogonal wavelets filter are employed for accurate detection of schizophrenia. The seven wavelet-based l_1 norm features are used for the classification of the schizophrenia and healthy subjects. In this work, the k-nearest neighbour classifier yielded the highest average classification accuracy of 99.21% using ten-fold cross-validation and 97.2% using leave-one-subject-out cross-validation. As we have used only single-channel Cz EEG, unlike other techniques, the proposed model is simple. We have got comparable classification performance (average accuracy more than 97%) when used ten-fold and leave-one-subject-out cross-validations as well as hold out validation. Hence, the suggested model is robust. Further, we have used only 7 seven features for the classification. The method is computationally lesser expensive than the existing methods. Our model has performed well in terms of all performance parameters, namely (average classification accuracy, Cohen's kappa value, and F1-score), which justifies the accuracy and robustness of the developed model. The proposed model can be used in a cloud-based system for online monitoring of schizophrenia. In the future, we intend to validate our model with some other diverse and big databases. We would also like to test our developed model to detect other mental conditions like epilepsy, depression, autism, and alcoholism.

Compliance with ethical standards

Conflict of interest The authors declare that they have no conflict of interest.

References

Acharya UR, Sree SV, Ang PCA, Yanti R, Suri JS (2012) Application of non-linear and wavelet based features for the automated identification of epileptic EEG signals. Int J Neural Syst 22(02):1250002

Acharya UR, Sudarshan VK, Adeli H, Santhosh J, Koh JE, Adeli A (2015) Computer-aided diagnosis of depression using EEG signals. Eur Neurol 73(5–6):329–336

Acharya UR, Fujita H, Oh SL, Raghavendra U, Tan JH, Adam M, Gertych A, Hagiwara Y (2018a) Automated identification of shockable and non-shockable life-threatening ventricular arrhythmias using convolutional neural network. Future Gener Comput Syst 79:952–959

Acharya UR, Oh SL, Hagiwara Y, Tan JH, Adeli H (2018b) Deep convolutional neural network for the automated detection and

diagnosis of seizure using EEG signals. Comput Biol Med 100:270–278
Acharya UR, Oh SL, Hagiwara Y, Tan JH, Adeli H, Subha DP (2018c) Automated EEG-based screening of depression using deep convolutional neural network. Comput Methods Programs Biomed 161:103–113
Akar SA, Kara S, Latifoğlu F, Bilgiç V (2012) Wavelet-welch methodology for analysis of EEG signals of schizophrenia patients. In: 2012 Cairo international biomedical engineering conference (CIBEC), pp 6–9
Bhati D, Sharma M, Pachori RB, Nair SS, Gadre VM (2016) Design of time-frequency optimal three-band wavelet filter banks with unit sobolev regularity using frequency domain sampling. Circuits Syst Signal Process 35(12):4501–4531
Bhurane AA, Dhok S, Sharma M, Yuvaraj R, Murugappan M, Acharya UR (2019a) Diagnosis of Parkinson's disease from electroencephalography signals using linear and self-similarity features. Expert Syst 13:e12472
Bhurane AA, Sharma M, San-Tan R, Acharya UR (2019b) An efficient detection of congestive heart failure using frequency localized filter banks for the diagnosis with ecg signals. Cogn Syst Res 55:82–94
Daubechies I (1992) Ten lectures on wavelets, vol 61. Siam, Philadelphia
De Winter JC (2013) Using the student's t-test with extremely small sample sizes. Pract Assess Res Eval 18(1):10
Devijver P, Kittler J (1982) Pattern recognition: a statistical approach. Prentice/Hall International, Upper Saddle River
Dhok S, Pimpalkhute V, Chandurkar A, Bhurane AA, Sharma M, Acharya UR (2020) Automated phase classification in cyclic alternating patterns in sleep stages using Wigner–Ville distribution based features. Comput Biol Med 119:103691
Dietterich TG (2000) An experimental comparison of three methods for constructing ensembles of decision trees: bagging, boosting, and randomization. Mach Learn 40(2):139–157
Dvey-Aharon Z, Fogelson N, Peled A, Intrator N (2015) Schizophrenia detection and classification by advanced analysis of EEG recordings using a single electrode approach. PLoS ONE 10(4):e0123033
Fushiki T (2011) Estimation of prediction error by using k-fold cross-validation. Stat Comput 21(2):137–146
Gudigar A, Raghavendra U, San TR, Ciaccio EJ, Acharya UR (2019) Application of multiresolution analysis for automated detection of brain abnormality using MR images: a comparative study. Future Gener Comput Syst 90:359–367
Ibáñez-Molina AJ, Lozano V, Soriano MF, Aznarte JI, Gómez-Ariza CJ, Bajo M (2018) Eeg multiscale complexity in schizophrenia during picture naming. Front Physiol 9:1213
Johannesen JK, Bi J, Jiang R, Kenney JG, Chen C-MA (2016) Machine learning identification of EEG features predicting working memory performance in schizophrenia and healthy adults. Neuropsychiat Electrophysiol 2(1):3
Kim JW, Lee YS, Han DH, Min KJ, Lee J, Lee K (2015) Diagnostic utility of quantitative EEG in un-medicated schizophrenia. Neurosci Lett 589:126–131
Laursen T, Nordentoft M, Brøbech P (2013) Excess early mortality in schizophrenia. Annu Rev Clin Psychol 10:425–448
Li Y, Tong S, Liu D, Gai Y, Wang X, Wang J, Qiu Y, Zhu Y (2008) Abnormal EEG complexity in patients with schizophrenia and depression. Clin Neurophysiol 119(6):1232–1241
Moulin P, Anitescu M, Kortanek KO, Potra FA (1997) The role of linear semi-infinite programming in signal-adapted qmf bank design. IEEE Trans Signal Process 45(9):2160–2174
Oh SL, Hagiwara Y, Raghavendra U, Yuvaraj R, Arunkumar N, Murugappan M, Acharya UR (2018a) A deep learning approach for Parkinson's disease diagnosis from EEG signals. Neural Comput Appl 32:10927–10933https://doi.org/10.1007/s00521-018-3689-5
Oh SL, Ng EY, San Tan R, Acharya UR (2018b) Automated diagnosis of arrhythmia using combination of cnn and lstm techniques with variable length heart beats. Comput Biol Med 102:278–287
Oh SL, Vicnesh J, Ciaccio EJ, Yuvaraj R, Acharya UR (2019) Deep convolutional neural network model for automated diagnosis of schizophrenia using EEG signals. Appl Sci 9(14):2870
Olejarczyk E, Jernajczyk W (2017) Graph-based analysis of brain connectivity in schizophrenia. PLoS ONE 12(11):e0188629
Rajendra SK, Shrimali M, Doshi S, Sharma M (2018) Detection of power transformer winding faults using orthogonal wavelet filter bank, pp 431–436
Rajput JS, Sharma M, Acharya UR (2019) Hypertension diagnosis index for discrimination of high-risk hypertension ecg signals using optimal orthogonal wavelet filter bank. Int J Environ Res Public Health 16(21):4068
Santos-Mayo L, San-José-Revuelta LM, Arribas JI (2016) A computer-aided diagnosis system with EEG based on the p3b wave during an auditory odd-ball task in schizophrenia. IEEE Trans Biomed Eng 64(2):395–407
Shah S, Sharma M, Deb D, Pachori, RB (2019) An automated alcoholism detection using orthogonal wavelet filter bank. In: 2019 International conference on machine intelligence and signal analysis advances in intelligent systems and computing, vol 748. Springer, Singapore, pp 473–483
Sharma M, Acharya UR (2018) Analysis of knee-joint vibroarthographic signals using bandwidth-duration localized three-channel filter bank. Comput Electr Eng 72:191–202
Sharma M, Acharya UR (2019) A new method to identify coronary artery disease with ecg signals and time–frequency concentrated antisymmetric biorthogonal wavelet filter bank. Pattern Recognit Lett 125:235–240
Sharma M, Pachori RB (2017) A novel approach to detect epileptic seizures using a combination of tunable-q wavelet transform and fractal dimension. J Mech Med Biol 17(07):1740003
Sharma M, Kolte R, Patwardhan P, Gadre V (2010) Time–frequency localization optimized biorthogonal wavelets. In: International conference on signal processing and communications (SPCOM) 2010, pp 1–5
Sharma M, Singh T, Bhati D, Gadre V (2014) Design of two-channel linear phase biorthogonal wavelet filter banks via convex optimization. In: 2014 International conference on signal processing and communications (SPCOM), pp 1–6
Sharma M, Gadre VM, Porwal S (2015) An eigenfilter-based approach to the design of time-frequency localization optimized two-channel linear phase biorthogonal filter banks. Circuits Syst Signal Process 34(3):931–959
Sharma M, Bhati D, Pillai S, Pachori RB, Gadre VM (2016) Design of time-frequency localized filter banks: transforming non-convex problem into convex via semidefinite relaxation technique. Circuits Syst Signal Process 35(10):3716–3733
Sharma M, Achuth PV, Pachori RB, Gadre VM (2017a) A parametrization technique to design joint time-frequency optimized discrete-time biorthogonal wavelet bases. Signal Process 135:107–120
Sharma M, Dhere A, Pachori RB, Acharya UR (2017b) An automatic detection of focal EEG signals using new class of time-frequency localized orthogonal wavelet filter banks. Knowl Based Syst 118:217–227
Sharma M, Dhere A, Pachori RB, Gadre VM (2017c) Optimal duration-bandwidth localized antisymmetric biorthogonal wavelet filters. Signal Process 134:87–99
Sharma M, Pachori RB, Acharya UR (2017d) A new approach to characterize epileptic seizures using analytic time-frequency

flexible wavelet transform and fractal dimension. Pattern Recognit Lett 94:172–179
Sharma M, Achuth P, Deb D, Puthankattil SD, Acharya UR (2018a) An automated diagnosis of depression using three-channel bandwidth-duration localized wavelet filter bank with EEG signals. Cogn Syst Res 52:508–520
Sharma M, Agarwal S, Acharya UR (2018b) Application of an optimal class of antisymmetric wavelet filter banks for obstructive sleep apnea diagnosis using ecg signals. Comput Biol Med 100:100–113
Sharma M, Bhurane AA, Acharya UR (2018c) MMSFL-OWFB: a novel class of orthogonal wavelet filters for epileptic seizure detection. Knowl Based Syst 160:265–277
Sharma M, Goyal D, Achuth P, Acharya UR (2018d) An accurate sleep stages classification system using a new class of optimally time-frequency localized three-band wavelet filter bank. Comput Biol Med 98:58–75
Sharma M, Sharma P, Pachori RB, Acharya UR (2018e) Dual-tree complex wavelet transform-based features for automated alcoholism identification. Int J Fuzzy Syst 20(5):1297–1308
Sharma M, Tan RS, Acharya UR (2018f) A novel automated diagnostic system for classification of myocardial infarction ecg signals using an optimal biorthogonal filter bank. Comput Biol Med 102:341–356
Sharma M, Patel S, Choudhary S, Acharya UR (2019a) Automated detection of sleep stages using energy-localized orthogonal wavelet filter banks. Arab J Sci Eng 45:2531–2544
Sharma M, Raval M, Acharya UR (2019b) A new approach to identify obstructive sleep apnea using an optimal orthogonal wavelet filter bank with ecg signals. Inform Med Unlocked 16:100170
Sharma M, Sing S, Kumar A, Tan RS, Acharya UR (2019c) Automated detection of shockable and non-shockable arrhythmia using novel wavelet-based ecg features. Comput Biol Med 115:103446
Sharma M, Tan R-S, Acharya UR (2019d) Automated heartbeat classification and detection of arrhythmia using optimal orthogonal wavelet filters. Inform Med Unlocked 16:100221
Sharma M, Tan R-S, Acharya UR (2019e) Detection of shockable ventricular arrhythmia using optimal orthogonal wavelet filters. Neural Comput Appl 32:15869–15884
Sharma M, Patel S, Acharya UR (2020) Automated detection of abnormal EEG signals using localized wavelet filter banks. Pattern Recognit Lett 133:188–194
Siuly S, Khare SK, Bajaj V, Wang H, Zhang Y (2020) A computerized method for automatic detection of schizophrenia using EEG signals. IEEE Trans Neural Syst Rehabil Eng 28(11):2390–2400
Subudhi A, Acharya UR, Dash M, Jena S, Sabut S (2018) Automated approach for detection of ischemic stroke using delaunay triangulation in brain mri images. Comput Biol Med 103:116–129
Sun S, Zhang C, Zhang D (2007) An experimental evaluation of ensemble methods for EEG signal classification. Pattern Recognit Lett 28(15):2157–2163
Talo M, Baloglu UB, Yıldırım Ö, Acharya UR (2019) Application of deep transfer learning for automated brain abnormality classification using mr images. Cogn Syst Res 54:176–188
Tay DB, Lin Z, Murugesan S (2014) Orthogonal wavelet filters with minimum RMS bandwidth. IEEE Signal Process Lett 21(7):819–823
Tomioka R, Aihara K, Müller K-R (2007) Logistic regression for single trial EEG classification. Adv Neural Inf Process Syst 19:1377–1384
Tripathy R, Acharya UR (2018) Use of features from RR-time series and EEG signals for automated classification of sleep stages in deep neural network framework. Biocybern Biomed Eng 38(4):890–902
Vetterli M, Herley C (1992) Wavelets and filter banks: theory and design. IEEE Trans Signal Process 40:2207–2232
Vicnesh J, Oh SL, Rajinikanth V, Ciaccio E, Cheong K, Arunkumar Acharya UR (2019) Automated detection of schizophrenia using nonlinear signal processing methods. Artif Intell Med 100:101698
Virdi P, Narayan Y, Kumari P, Mathew L (2016, July). Discrete wavelet packet based elbow movement classification using fine Gaussian SVM. In: 2016 IEEE 1st international conference on power electronics, intelligent control and energy systems (ICPEICES), pp 1–5
Wang H, Lu X, Hu Z, Zheng W (2014) Fisher discriminant analysis with l1-norm. IEEE Trans Cybern 44(6):828–842
Xu Y, Zhu Q, Fan Z, Qiu M, Chen Y, Liu H (2013) Coarse to fine k nearest neighbor classifier. Pattern Recognit Lett 34(9):980–986
Yıldırım Ö, Baloglu UB, Acharya UR (2018) A deep convolutional neural network model for automated identification of abnormal EEG signals. Neural Comput Appl 32:15857–15868